Proceedings of the
Annual Stability Conference
Structural Stability Research Council
Louisville, Kentucky, April 1-4, 2025

Flexural-torsional buckling of built-up cold-formed steel columns

Kim J.R. Rasmussen[1], M. Khezri[2]

Abstract
The paper presents analytical solutions to the buckling of singly symmetric built-up CFS sections, for which the critical mode may be flexural-torsional. The derivation treats the fasteners as discrete since often, they are not installed sufficiently close that accurate solutions can be obtained by smearing the fastener shear stiffness over the length of the column. The derivation is based on an elastic energy solution that adds the strain energy of the fasteners to the strain energy of the component sections. Solutions are obtained for simply supported end conditions considering both loading through ball bearings that allow free warping displacements and loading through rigid end platens that prevent warping. A parametric study is presented to explain the influence of the number of discrete fasteners on the buckling load of singly symmetric columns buckling in the flexural-torsional mode. The optimal location of fasteners for pin-ended columns buckling in the flexural-torsional mode is also explained.

1. Introduction

Built-up cold-formed steel sections are finding increasing use in Australia, North America and Europe because of opportunity to greatly enhance the global buckling capacity by increasing the flexural, torsional and warping rigidities through joining two or more cross-sections. Built-up sections offer great versatility in creating innovative shapes with superior properties, e.g. several singly symmetric cross-sections may be joined to create a doubly symmetric built-up section, or several open sections may be joined to create a built-up sections with a closed loop and associated enhanced torsional rigidity (GJ). Because of the enhanced global buckling capacity, built-up sections are now being used as primary structural members of mid-rise residential buildings and large-span portal frames.

Numerous investigations of the strength and behaviour of cold-formed steel built-up sections have been published over the last two decades on doubly symmetric columns featuring two component sections, mainly two back-to-back C-sections featuring flat webs and webs stiffened with small intermediate stiffeners or large stiffeners producing a closed loop in the built-up configuration (Zhang and Young 2015, Lu et al. 2017, Fratamico et al. 2018, Roy et al. 2018, Chen et al. 2020, Zhou et al. 2020, Li and Young 2022, Mahar et al. 2023, Yang et al. 2024). Being doubly

[1] Professor, University of Sydney, <kim.rasmussen@sydney.edu.au>
[2] Senior Lecturer, University of Sydney, <mani.khezri@sydney.edu.au>

symmetric, the built-up columns failed by flexure in the global mode. Further investigation of the use of closed loops was presented by Meza et al. (2020) who tested four distinct built-up cross-sections composed of combinations of plain and lipped channel sections with flat plates. Up to four component sections were employed to create the built-up sections, all doubly symmetric and failing flexurally in the global mode.

The buckling behaviour of singly symmetric built-up cold-formed steel columns has been investigated by Georgieva et al. (2012) and Phan et al. (2019, 2021, 2022). In Georgieva, Schueremans et al. (2012), two equal Z-sections were connected through the lips to create a singly symmetric hat section, whereas in Phan et al. (2019, 2021, 2022), three component lipped channel sections were combined, two back-to-back with the third connected through the web to the flanges of the back-to-back pair. The critical global buckling mode of both built-up cross-sections was the flexural-torsional mode. More recently, Dobric et al. (2024) published a study of built-up cold-formed columns featuring a complex cruciform cross-section with lip-stiffened legs composed of six plain channel sections. Being point symmetric, the critical global mode was the torsional mode.

Current Australian and North American specifications for cold-formed steel structures (AS/NZS4600 2018, AISI-S100 2020) have provisions for back-to-back built-up columns failing by flexural buckling, comprising a modified slenderness to account for the lack of full-partial composite action in the built-up column. The specifications also enforce a maximum fastener spacing to prevent buckling from occurring between fastener stations. However, the specifications do not have provisions for built-up columns with cross-sections other than back-to-back channel sections. In particular, they do not provide guidance on the design of singly and point symmetric columns failing globally in flexural-torsional and torsional modes. Design provisions were proposed in (Phan, Rasmussen et al. 2022) for the design of singly symmetric columns, in which the modified slenderness approach was combined with the classical flexural-torsional buckling equation (Trahair 1993),

$$P_{cr} = \frac{P_y + P_z - \sqrt{\left(P_y + P_z\right)^2 - 4P_y P_z \left(1 - \left(\frac{y_S}{r_2}\right)^2\right)}}{2\left(1 - \left(\frac{y_S}{r_2}\right)^2\right)}, \tag{1}$$

in which P_y and P_z are the major axis flexural buckling load and torsional buckling load, respectively, y_S is the distance between the centroid and the shear centre and r_2 is the polar radius of gyration with respect to the shear centre.

2. Theoretical derivations

2.1 General

We consider the buckling of singly symmetric built-up section columns, i.e. built-up cross-sections with a single axis of symmetry, for which the critical buckling modes are a pure flexural mode in the plane of symmetry and two flexural-torsional modes with flexure occurring in the plane perpendicular to the axis of symmetry (Trahair 1993). Solutions to the flexural buckling of doubly, singly and point symmetric built-up section columns are presented in (Rasmussen et al. 2020). In the present paper, we pursue solutions to buckling in the flexural-torsional modes.

In deriving equations for the flexural-torsional buckling load of such columns, we pay attention to the end support conditions and their influence on the effectiveness of fasteners to provide composite action. We expand the general framework presented in (Rasmussen et al. 2020) for determining the flexural buckling load to flexural-torsional buckling in Section 2.2 and subsequently apply the framework to the flexural-torsional buckling of columns composed of two sections considering various support conditions in Section 3.

In deriving the buckling equations, we take the discrete locations of fasteners into account, rather than accounting for partial composite action by smearing the effect of fasteners into a constant continuous shear stiffness, as is commonly done in the literature. The advantage of this approach is that it allows the influences of support conditions and mode of deformation on the shear deformations at fastener points to be accurately accounted for.

It is noted that in addition to checking the flexural-torsional column buckling strength, which is the focus of this paper, the design of singly-symmetric cold-formed steel built-up columns to the Australian and American specifications (AS/NZS4600 2018, AISI-S100 2020) also requires the flexural buckling in the plane of symmetry and the local and distortional buckling capacities (Abbasi et al. 2023) to be checked.

2.2 Kinematics

We consider a cross-section composed of two or more individual sections connected by discrete fasteners, as shown in Fig. 1. The component sections and fasteners are assumed to be arranged to produce a singly symmetric cross-section such that the centroid (C) and shear centre (S) are located on the symmetry axis. A Cartesian system with origin at the centroid is chosen for the coordinates (x,y,z). Assuming the shear deformations of the fasteners are small compared to the dimensions of the component sections, the locations of the centroid and shear centre can be obtained assuming the cross-section is fully composite (Rasmussen et al. 2020).

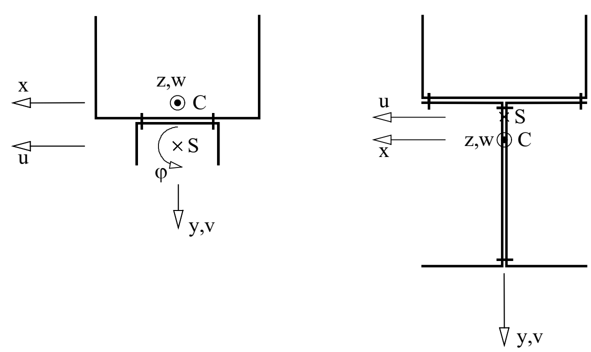

Figure 1: Built-up cross-section, coordinate system and generalised displacements for members with (a) two component sections and (b) three component sections

Cartesian systems are also introduced to define the points and displacements of each component section, as shown in Fig. 2b. The superscript m_k is introduced to refer to the m_k'th component section, such that (x^{m_k}, y^{m_k}, z^{m_k}), (u^{m_k}, v^{m_k}, w^{m_k}), C^{m_k} and S^{m_k} are the coordinates, generalised displacements in the (x^{m_k}, y^{m_k}, z^{m_k}) directions, centroid and shear centre of the m_k'th section, respectively. All sections share the same z-coordinate, i.e. $z^{m_k} = z$, and depending on the location of the centroids of the component sections, several sections may share the same x^{m_k} or y^{m_k} coordinate, which may also coincide with the x- or y-coordinate.

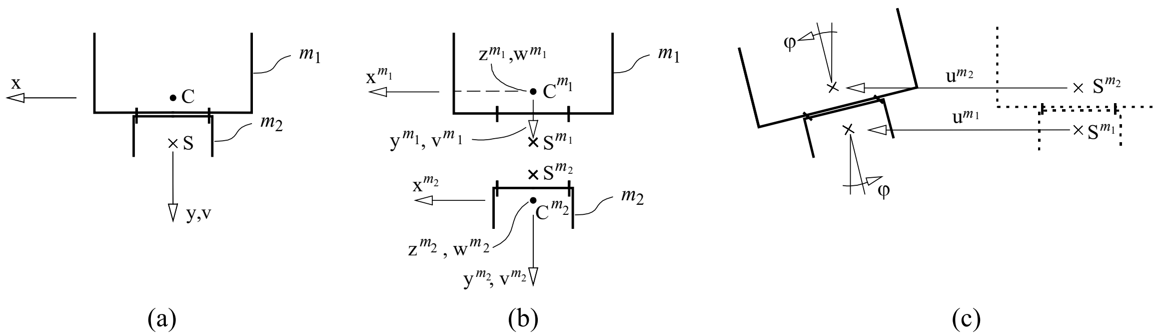

Figure 2: a) Component sections, b) coordinate systems and c) generalised displacements

Because the built-up section is singly symmetric, the global buckling modes comprise a pure flexural mode in the plane of symmetry and two flexural-torsional modes, of which the latter are the subject of this paper. In the flexural-torsional modes, flexure occurs in the x-direction perpendicular to the plane of symmetry, i.e. $v^{m_k} = 0$. The fasteners are assumed to be flexible in shear but rigid axially, so that the relative displacement between component sections consist of only longitudinal and transverse displacements in the plane of abutting surfaces, as shown in Fig. 2c. It follows that all component sections have the same twist rotation (φ). The flexural displacements of the component sections (u^{m_k}) will be different when shear deformations of fasteners allow differential flexural displacements of the sections.

Fasteners are assumed to be installed at discrete fastener stations (z_i, $i = 1, 2, \ldots, n_{fl}$), where n_{fl} is the number of fastener stations along the length. At each fastener station, n_{ft} fasteners are installed in the cross-section, each referred to by the index $j = 1, 2, \ldots, n_{ft}$, as shown in Fig. 3. The cross-sectional locations of the fastener are assumed to be identical at each fastener station. The total shear deformation of the (i,j)'th fastener is referred to as Δ_{ij}. It comprises a longitudinal and a transverse component, referred to as $\Delta_{l,ij}$ and $\Delta_{t,ij}$, respectively, as shown in Fig. 3. The shear deformations ($\Delta_{l,ij}$, $\Delta_{t,ij}$) can be expressed in terms of the generalised displacements and the coordinates of the fastener points, as demonstrated in Section 3.1.

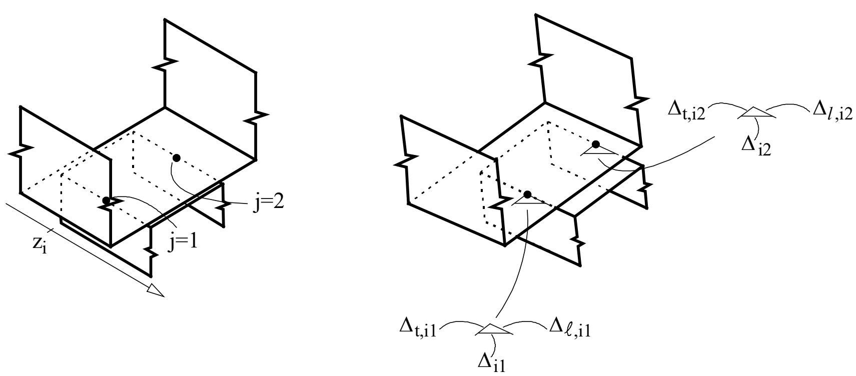

Figure 3: Fastener locations and shear displacements of fasteners

2.3 Virtual work equation

We establish the flexural-torsional buckling equation using a virtual work approach. In so doing, the virtual work of the component beams is readily expressed using Bernoulli beam theory as in (Rasmussen et al. 2020) and well-established equations for the bifurcation of thin-walled members. For the latter, the virtual work formulation presented in (Rasmussen 1997) is chosen which is based on the perturbation theory set out in (Budiansky 1974).

To the virtual internal work done by the component sections ($\sum \delta W_i^{m_k}$), we add the virtual work done by the fasteners (δW_{if}), i.e.

$$\delta W_i = \sum_{k=1}^{n_m} \delta W_i^{m_k} + \delta W_{if} \ , \tag{2}$$

where n_m is the number of component sections, and

$$\delta W_{if} = \sum_{i=1}^{n_{fl}} \sum_{j=1}^{n_{ft}} F_{s,ij} \delta \Delta_{ij}, \tag{3}$$

The shear force at the (i,j)'th fastener point ($F_{s,ij}$) is given by,

$$F_{s,ij} = k_{ij} \Delta_{ij}, \tag{4}$$

where k_{ij} is the shear stiffness of the (i,j)'th fastener. The shear deformation can be expressed as

$$\Delta_{ij} = {}^{0}\Delta_{ij} + \dot{\Delta}_{ij}, \tag{5}$$

in which the prescript "0" and the accent "·" indicate quantities on the fundamental path and bifurcated path respectively. We will assume the built-up column is uniformly compressed whereby the shear deformation of fasteners is zero on the fundamental path, (${}^{0}\Delta_{ij} = 0$), and so,

$$\Delta_{ij} = \dot{\Delta}_{ij}. \tag{6}$$

In expressing equilibrium on the bifurcated path, the virtual work equation is divided by the norm of a characteristic buckling displacement ($\|u\|$) and considered in the limit $\lambda \to \lambda_{cr}$, where λ is a load factor and λ_{cr} its critical value. This leads to the following expression for the internal virtual work of the m_k'th component section,

$$\begin{aligned} \delta\, {}^{b}W_i^{m_k} &= \int_L \left(EA^{m_k}\, {}^{b}w^{m_k\prime}\, \delta w^{m_k\prime} + EI_y^{m_k}\, {}^{b}u^{m_k\prime\prime}\, \delta u^{m_k\prime\prime} + EI_\omega^{m_k}\, {}^{b}\varphi^{\prime\prime}\, \delta\varphi^{\prime\prime} \right. \\ &\quad \left. + GJ^{m_k}\, {}^{b}\varphi^{\prime}\, \delta\varphi^{\prime} \right) \mathrm{d}z + {}^{0}N_{cr}^{m_k} \int_L \left({}^{b}u^{m_k\prime}\, \delta u^{m_k\prime} + y_S^{m_k}\, {}^{b}u^{m_k\prime}\, \delta\varphi^{\prime} \right. \\ &\quad \left. + y_S^{m_k}\, {}^{b}\varphi^{\prime}\, \delta u^{m_k\prime} + \left(\left(y_S^{m_k}\right)^2 + \frac{I_P^{m_k}}{A^{m_k}} \right) {}^{b}\varphi^{\prime}\, \delta\varphi^{\prime} \right) \mathrm{d}z \ , \end{aligned} \tag{7}$$

in which the prescript "b" indicates a quantity on the bifurcated path, E and G are the elastic and shear moduli, respectively, $(A^{m_k}, I_y^{m_k}, I_\omega^{m_k}, J^{m_k})$ are the area, second moment of area about the y-axis, warping constant and torsion constant, respectively, $y_S^{m_k}$ is the distance from the centroid (C^{m_k}) to the shear centre (S^{m_k}), $I_P^{m_k}$ is the polar moment of area, i.e.

$$I_P^{m_k} = \int_{A^{m_k}} (x^2 + y^2)\, dA^{m_k} = I_x^{m_k} + I_y^{m_k}, \tag{8}$$

and ${}^0N_{cr}^{m_k}$ is the axial force acting on the m_k'th section at the point of buckling, positive as tensile. Introducing the buckling stress, σ_{cr}, the buckling load on the m_k'th section $(P_{cr}^{m_k})$ and the total buckling load of the built-up column (P_{cr}) are given by,

$$P_{cr}^{m_k} = -\ {}^0N_{cr}^{m_k} = A^{m_k}\sigma_{cr}, \text{ and} \tag{9}$$

$$P_{cr} = \sum_{k=1}^{n_m} P_{cr}^{m_k} = A\sigma_{cr}, \tag{10}$$

respectively, where

$$A = \sum_{k=1}^{n_m} A^{m_k}, \tag{11}$$

is the total area.

Defining the buckling shear deformation of the (i,j)'th fastener by (Budiansky 1974),

$${}^b\Delta_{ij} = \lim_{\lambda \to \lambda_{cr}} \frac{\dot{\Delta}_{ij}}{\|u\|}\ , \tag{12}$$

the virtual internal work done by the fasteners on the bifurcated path reduces to,

$$\delta\ {}^bW_{if} = \sum_{i=1}^{n_{fl}} \sum_{j=1}^{n_{ft}} k_{f,ij}\ {}^b\Delta_{ij}\ \delta\Delta_{ij}\ . \tag{13}$$

The virtual external work of the bifurcated path $(\delta\ {}^bW_e)$ is associated with a quadratic operator on the displacements at the loading points, and so vanishes for a column in uniform compression, for which the external work is linearly related to the axial displacement (Rasmussen 1997), i.e.

$$\delta\ {}^bW_e = 0\ . \tag{14}$$

Consequently, the virtual work equation for calculating the buckling load can be expressed as,

$$\sum_{k=1}^{n_m} \int_L \left(EA^{m_k}\, w^{m_k\prime}\, \delta w^{m_k\prime} + EI_y^{m_k}\, u^{m_i\prime\prime}\, \delta u^{m_k\prime\prime} + EI_\omega^{m_k} \varphi''\, \delta\varphi'' + GJ^{m_k}\varphi'\, \delta\varphi' \right) dz$$
$$- \sigma_{cr} \sum_{k=1}^{n_m} A^{m_k} \int_L \left(u^{m_k\prime}\, \delta u^{m_k\prime} + y_S^{m_k}\, u^{m_k\prime}\, \delta\varphi' + y_S^{m_k}\varphi'\, \delta u^{m_k\prime} \right.$$

$$+\left(\left(y_S^{m_k}\right)^2+\frac{I_P^{m_k}}{A^{m_k}}\right)\varphi'\,\delta\varphi'\Bigg)\Bigg)\mathrm{d}z+\sum_{i=1}^{n_{fl}}\sum_{j=1}^{n_{ft}}k_{f,ij}\Delta_{ij}\,\delta\Delta_{ij}=0\,, \qquad (15)$$

where, for simplicity, the prescript "b" has been dropped as it understood that *all* quantities in Eq. (15) are associated with the bifurcated path, except for σ_{cr}.

Solving Eq. (15) is challenging because of the discrete term in Δ_{ij}, which requires the segments between fasteners to be considered individually and leads to a large number of simultaneous equations for an exact solution. Hence an approximate energy solution is pursued in the following section.

2.4 Approximate solution for the buckling load

Because of the effort required to obtain exact solutions, we pursue an approximate approach which will be demonstrated to be accurate. For this, we use an assumed expression for the buckling field (u^{m_k}, φ), i.e.

$$u^{m_k}=\sum_{l=1}^{L}A_l^{u^{m_k}}\,f_l^{u^{m_k}}(z) \quad , \quad \varphi=\sum_{l=1}^{L}A_l^{\varphi}\,f_l^{\varphi}(z) \qquad (16)$$

where $A_l^{u^{m_k}}$ and A_l^{φ} are the amplitudes of the lth functions $f_l^{u^{m_k}}(z)$ and $f_l^{\varphi}(z)$, respectively, and L is the number of terms. Because the buckling field (u^{m_k}, φ) can now be assumed to be known, it is possible to calculate the corresponding shear forces transferred by the fasteners, as set out in Section 3.1. As they are the shear forces developing on the bifurcated path in the limit $\lambda\to\lambda_{cr}$, they are infinitesimal and can be obtained from linear theory. Accordingly, they are linear in the amplitudes ($A_l^{u^{m_k}}$, A_l^{φ}). Once the fastener shear forces are found, the axial forces ($N_i^{m_k}$) in each component section (m_k) in each segment (i) between fasteners stations can be obtained by equilibrium. These axial forces are generated by the transfer of shear forces between component sections and appear in the buckling equation (15) through the first term, *viz*.

$$N_i^{m_k}=EA^{m_k}\,w^{m_k\prime}. \qquad (17)$$

By use of Eq. (4), having found the fastener shear forces also allows the fastener shear deformations (Δ_{ij}) appearing in the last term of the buckling equation to be obtained. Since the fastener shear forces are liner in the amplitudes ($A_l^{u^{m_ik}}$, A_l^{φ}), so are the axial forces ($N_i^{m_k}$) and the shear deformations (Δ_{ij}). Hence all real terms in the buckling equation (15) are linear in the amplitudes.

The virtual displacement field is chosen affine to the real displacement field, as follows,

$$\delta u^{m_k}=\sum_{l=1}^{L}\delta A_l^{u^{m_k}}\,f_l^{u^{m_k}}(z) \quad , \quad \delta\varphi=\sum_{l=1}^{L}\delta A_l^{\varphi}\,f_l^{\varphi}(z)\ . \qquad (18)$$

It follows that the virtual shear forces, virtual axial forces ($\delta N_i^{m_k}$) and virtual fastener shear deformations ($\delta\Delta_{ij}$) can be obtained from the solutions for the corresponding real quantities by substituting the real amplitudes ($A_l^{u^{m_k}}$, A_l^{φ}) by the virtual amplitudes ($\delta A_l^{u^{m_k}}$, δA_l^{φ}). The virtual axial strain ($\delta w^{m_k\prime}$), can then be obtained from,

$$\delta w^{m_k\prime} = \frac{\delta N_i^{m_k}}{EA^{m_k}} \, . \tag{19}$$

It follows that all virtual quantities in Eq. (15) are linear in the virtual amplitudes ($\delta A_l^{u^{m_k}}$, δA_l^{φ}) and that all terms are products of a real and a virtual quantity. Hence the buckling equation can be ordered as,

$$\begin{gathered}\{K_{1,1} \quad \cdots \quad K_{1,(n_m+1)L}\}\begin{Bmatrix} A_1^{u^{m_1}} \\ \vdots \\ A_L^{\varphi} \end{Bmatrix}\delta A_1^{u^{m_1}} + \cdots + \\ \{K_{(n_m+1)L,1} \quad \cdots \quad K_{(n_m+1)L,(n_m+1)L}\}\begin{Bmatrix} A_1^{u^{m_1}} \\ \vdots \\ A_L^{\varphi} \end{Bmatrix}\delta A_L^{\varphi} = 0 \ , \end{gathered} \tag{20}$$

where the coefficient to each virtual amplitude must vanish because the virtual amplitudes are arbitrary. The resulting (n_m+1)·L equations can be arranged as follows,

$$\begin{bmatrix} K_{1,1} & \cdots & K_{1,(n_m+1)L} \\ \vdots & \ddots & \vdots \\ K_{(n_m+1)L,1} & \cdots & K_{(n_m+1)L,(n_m+1)L} \end{bmatrix}\begin{Bmatrix} A_1^{u^{m_1}} \\ \vdots \\ A_L^{\varphi} \end{Bmatrix} = \begin{Bmatrix} 0 \\ \vdots \\ 0 \end{Bmatrix} . \tag{21}$$

Non-trivial solutions require the determinant of the coefficient matrix is zero, i.e.

$$\begin{vmatrix} K_{1,1} & \cdots & K_{1,(n_m+1)L} \\ \vdots & \ddots & \vdots \\ K_{(n_m+1)L,1} & \cdots & K_{(n_m+1)L,(n_m+1)L} \end{vmatrix} = 0 \ , \tag{22}$$

from which the buckling stress (σ_{cr}) can be determined. The buckling load (P_{cr}) then follows from Eq. (10).

3. Flexural-torsional buckling of built-up section comprising two unequal plain channel sections

3.1 Axial forces and fastener shear forces associated with buckling

We consider the built-up section shown in Fig. 2a comprising two plain channel sections of unequal size. The buckling displacements of the two sections in the transverse and longitudinal directions are shown in Fig. 4a and Fig. 4b respectively. Observing that u^{m_1} and u^{m_2} are the displacements of the shear centres of m_1 and m_2, respectively, it follows that the buckling displacements at the fastener points can be obtained as,

$$u_{ij}^{m_1} = u^{m_1} + \varphi d_S^{m_1} \quad , \quad w_{ij}^{m_1} = -u^{m_1\prime} x_j^{m_1} - \varphi' \omega_j^{m_1} \tag{23}$$

$$u_{ij}^{m_2} = u^{m_2} - \varphi d_S^{m_2} \quad , \quad w_{ij}^{m_2} = -u^{m_2\prime} x_j^{m_2} - \varphi' \omega_j^{m_2} , \tag{24}$$

where $x_1^{m_1} = x_1^{m_2} = b_w^{m_2}/2$, $x_2^{m_1} = x_2^{m_2} = -b_w^{m_2}/2$, $d_S^{m_1}$ and $d_S^{m_2}$ are the distances from the shear centre to the web of sections m_1 and m_2, respectively, and $\omega_j^{m_k}$is the sectorial coordinate of section m_k at fastener point j. The shear deformations of the fasteners in the transverse ($\Delta_{t,ij}$) and longitudinal ($\Delta_{l,ij}$) directions can be calculated as,

$$\Delta_{t,ij} = u_{ij}^{m_2} - u_{ij}^{m_1} \quad \text{and} \quad \Delta_{l,ij} = w_{ij}^{m_2} - w_{ij}^{m_1} \,, \tag{25}$$

respectively, which on substitution of Eqs (23, 24) produce,

$$\Delta_{t,ij} = u^{m_2} - u^{m_1} - \varphi(d_S^{m_2} + d_S^{m_1}) \,, \tag{26}$$

$$\Delta_{l,ij} = -\left(u^{m_2\prime} x_j^{m_2} - u^{m_1\prime} x_j^{m_1}\right) - \varphi'(\omega_j^{m_2} - \omega_j^{m_1}) \,. \tag{27}$$

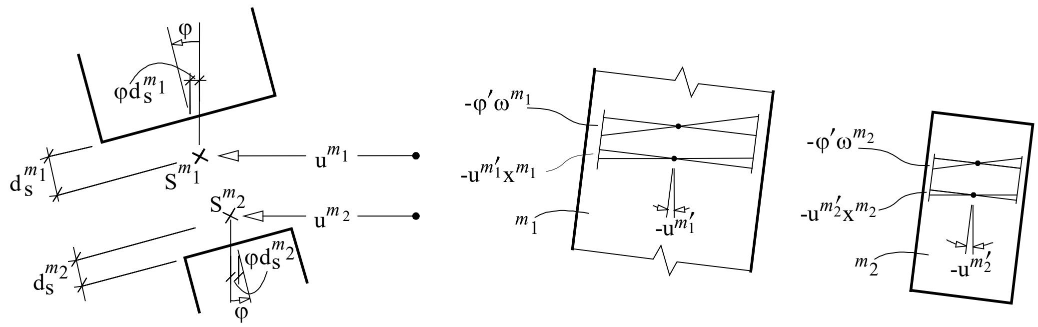

(a) Elevation, exploded view

(b) Plan, exploded view

Figure 4: Displacements in the (a) transverse and (b) longitudinal directions

It follows from Eq. (4) that the fastener shear forces in the transverse and longitudinal directions (Fig. 5a) are given by,

$$F_{st,ij} = k_{ij}\Delta_{t,ij} \,, \tag{28}$$

$$F_{sl,ij} = k_{ij}\Delta_{l,ij} \,. \tag{29}$$

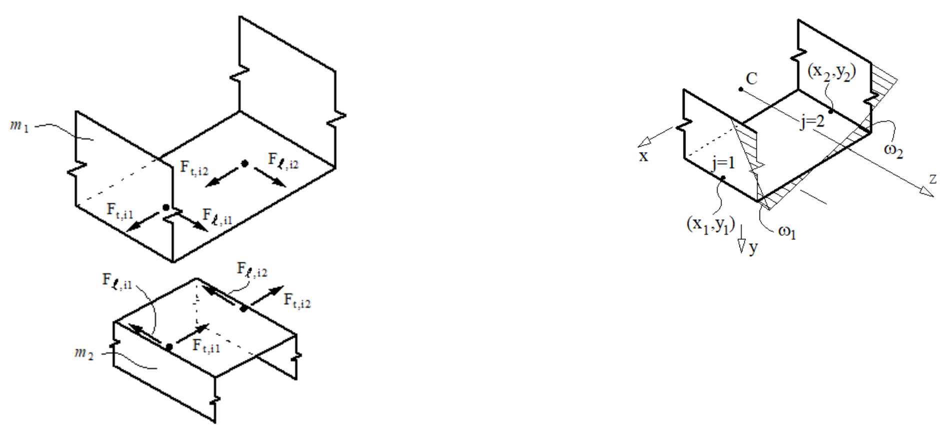

(a)

(b)

Figure 5: (a) fastener shear forces and (b) sectorial coordinate (ω)

Consider now fastener station (i), the total longitudinal shear forces transferred by the fasteners to the component sections are,

$$\bar{N}_i^{m_1} = \sum_{j=1}^{n_{ft}} F_{l,ij} \tag{30}$$

$$\bar{N}_i^{m_2} = -\sum_{j=1}^{n_{ft}} F_{l,ij}, \tag{31}$$

where $\bar{N}_i^{m_1}$ and $\bar{N}_i^{m_2}$ are positive in the z-direction.

Because the two channel sections are symmetric about the y-axis, it follows that $x_1^{m_1}$=-$x_2^{m_1}$, $x_1^{m_2}$=-$x_2^{m_2}$, $\omega_1^{m_1}$=-$\omega_2^{m_1}$ and $\omega_1^{m_2}$=-$\omega_2^{m_2}$. On substituting these relations into Eq. (27) and combining Eqs (27, 29-31), it follows that for the section shown in Fig. 2a, the longitudinal shear forces transferred at each fastener station is identically zero,

$$\bar{N}_i^{m_1} = \bar{N}_i^{m_2} = 0\,, \tag{32}$$

i.e. the axial forces (N^{m_k}) in each component channel section resulting from the buckling displacements are constant along the length of the column. In physical terms, for each component section, the longitudinal shear forces at the two fastener points are equal but in opposite directions ($F_{l,i1}$=-$F_{l,i2}$) so that the resultant force is zero. Note that this is not a general result for the flexural-torsional buckling of singly symmetric built-up sections. It is a result of the fact that the fasteners are located on a plane parallel to the plane of major axis flexural buckling. Sections with fasteners located on a plane perpendicular to the plane of major axis flexural buckling, such as that shown in Fig. 1b, will develop self-equilibrating axial forces in the component sections during buckling.

3.2 Solution for a simply supported built-up column with each channel section free to warp at the ends

We consider the simply supported built-up column shown in Fig. 6. The length of the column is L = 2000mm and the ends free to warp. The elastic modulus is E = 200,000 MPa. The cross-section dimensions are shown in Fig. 7.

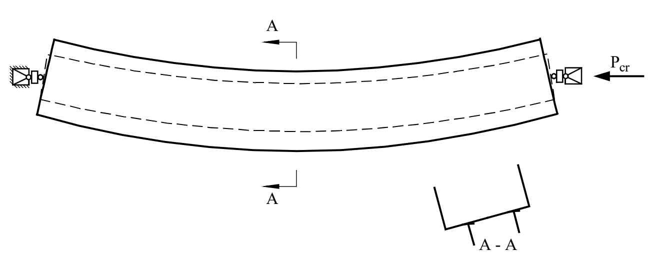

Figure 6: Simply supported column with ends free to warp

As shown in Fig. 7, at each longitudinal fastener station (i), fasteners between the webs are installed at the flange-web junctions of the smaller component section. All fasteners are assumed to have the same shear stiffness (k), i.e. $k_{ij} = k$.

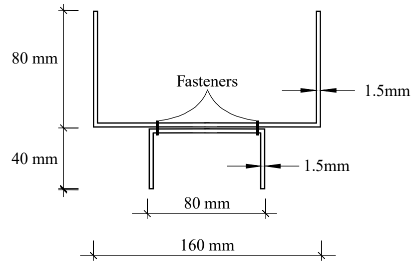

Figure 7: Dimensions and fastener points of built-up cross-section

At the supports, the applied load is transferred to the cross-sections of the component sections using a linkage and ball bearings that allow the sections to rotate freely and independently about the major axis, as shown in Fig. 8.

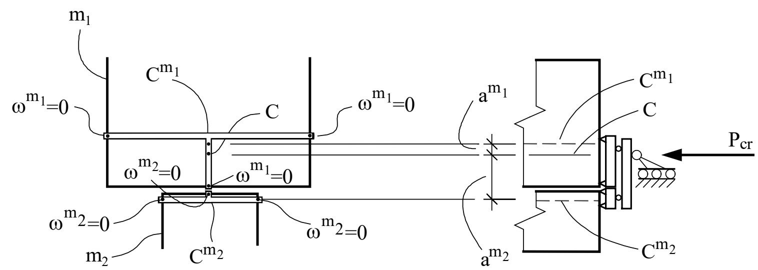

a) Free to warp loading arrangement

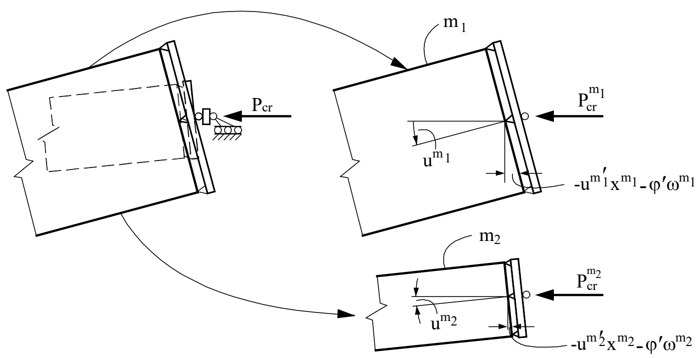

b) Warping and in-plane flexural displacements at supports

Figure 8: Free to warp support conditions using pinned linkage

The ball bearings are aligned with the centroids of the respective component sections to ensure the component beams are uniformly compressed until reaching the buckling load (P_{cr}). The load is applied through the centroid of the built-up section, whereby the distances (a^{m_1}, a^{m_2}) from the line of action of the applied load to the load application points of the component sections, as shown in Fig. 8a, are given by,

$$a^{m_1} = \frac{A^{m_1}}{A^{m_1}+A^{m_2}}\left(d_C^{m_1} + d_C^{m_2}\right) \tag{33}$$

$$a^{m_2} = \frac{A^{m_2}}{A^{m_1}+A^{m_2}}\left(d_C^{m_1} + d_C^{m_2}\right) . \tag{34}$$

Because of the pinned arrangement, the component sections are free to displace axially at the ends and axial forces cannot be transferred during buckling from one section to the other, as shown in Fig. 9. It follows that the axial forces at the end cross-sections of the component beams developing during buckling are zero ($N^{m_1}(0) = N^{m_2}(0) = N^{m_1}(L) = N^{m_2}(L) = 0$).

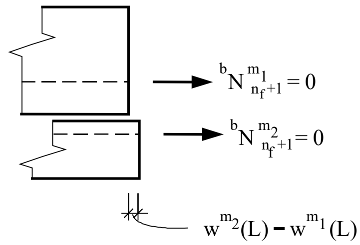

Figure 9: Side view of axial forces and relative longitudinal displacements at end cross-sections. Loading through linkage and ball bearings

Combined with the fact that no net axial forces are transferred between the component sections at the fastener stations (Eq. (32)), it follows that no axial forces develop during buckling, i.e. the axial forces ($N_i^{m_k}$) in all segments (i) between fasteners stations are zero. Consequently, the first term ($EA^{m_k}\, w^{m_k\prime}\, \delta w^{m_k\prime}$) of the energy equation (Eq. (15)) vanishes.

The solution is obtained for the following displacement field,

$$u^{m_1}(z) = A_{u1}^{m_1} \sin\left(\frac{\pi z}{L}\right) \tag{35}$$

$$u^{m_2}(z) = A_{u1}^{m_2} \sin\left(\frac{\pi z}{L}\right) \tag{36}$$

$$\varphi(z) = A_{\varphi 1} \sin\left(\frac{\pi z}{L}\right), \tag{37}$$

which satisfies the end support conditions and is the exact solution for the fully composite built-up section. Solutions for the buckling load (P_{cr}) are obtained for a single fastener station at mid-length, two fastener stations at the ends and 3, 4, 5 and 6 equidistant fastener stations, as shown schematically in Fig. 10.

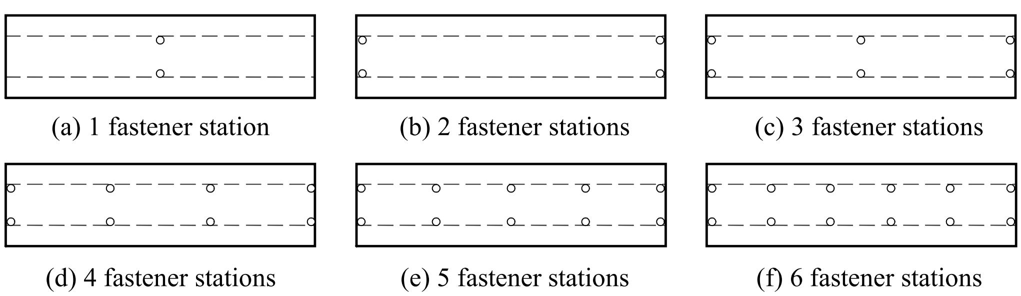

(a) 1 fastener station (b) 2 fastener stations (c) 3 fastener stations

(d) 4 fastener stations (e) 5 fastener stations (f) 6 fastener stations

Figure 10: Longitudinal fastener arrangements

The buckling loads are shown in Fig. 11, normalised with respect to the buckling load ($P_{\mathrm{cr}}(k{=}0)$) for the case of no fasteners, for which the component sections are free to slide along the interface between the webs in both the longitudinal and transverse directions, while maintaining the same twist rotation. The buckling loads are shown against the relative fastener shear stiffness ($\bar{k}$),

$$\bar{k} = \frac{k}{\frac{EA^{m1}}{L}} \quad . \tag{38}$$

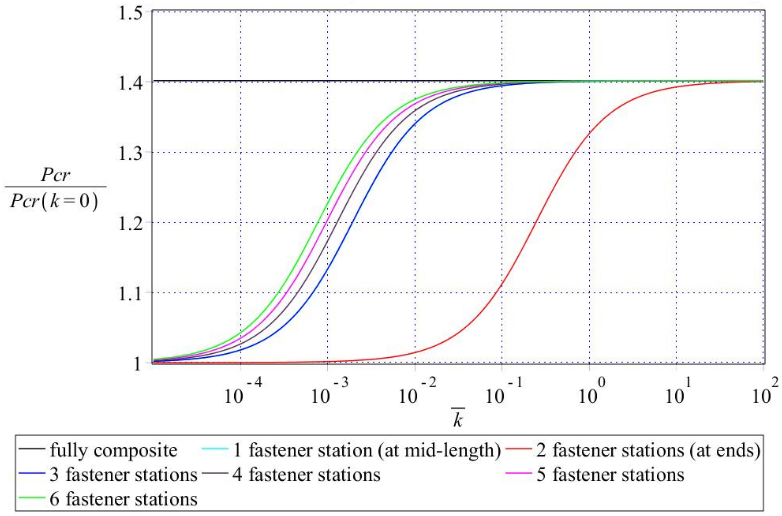

Figure 11: Nondimensional buckling load for simply supported built-up column with ends free to warp, ($P_{cr}(k=0) = 130.3$ kN)

It follows from Fig. 11 that the buckling load increases as the number of fastener stations increases, except for the case of two fastener stations, for which a substantially higher shear stiffness is required to achieve the buckling loads of other fastener arrangements. This is because for fastener arrangements other than two end fastener stations, the increase in buckling load is mobilised by the transverse shear stiffness at fastener stations along the length of the column, and, given the relatively high lateral flexibility of the component sections, only a relatively small stiffness ($\bar{k} \approx 10^{-1}$) is required to provide effectively full composite action. Conversely, in the case of two fastener stations at the ends, composite action is mobilised solely by the longitudinal shear stiffness of the fasteners and the relative warping displacements of the component sections at the fastener points. These relative warping displacements are an order of magnitude smaller than the relative transverse shear deformations along the length of the member, and hence much greater shear stiffness is required to achieve the same level of composite action. For the same reason, the end fasteners contribute negligibly to the increase in buckling load compared to the fasteners along the length and hence, the solutions for one and three fastener stations are indistinguishable in Fig. 11. Note that the shear stiffness of fasteners typically used in practice lie in the range $\bar{k} \in [10^{-1}, 10^{+1}]$ and hence, only a few fasteners are required along the length to achieve full composite action.

For all fastener arrangements, under increasing fastener shear stiffness, the buckling load asymptotes to the value ($P_{cr} = 182.5$ kN) obtained using Eq. (1), corresponding to full composite action. The solution is thus accurate in the limit $\bar{k} \to \infty$. To check the accuracy of the solution for finite values of $\bar{k}$, a second term was added to the displacement field as follows,

$$u^{m_1}(z) = A_{u1}^{m_1} \sin\left(\frac{\pi z}{L}\right) + A_{u3}^{m_1} \sin\left(\frac{3\pi z}{L}\right) \tag{39}$$

$$u^{m_2}(z) = A_{u1}^{m_2} \sin\left(\frac{\pi z}{L}\right) + A_{u3}^{m_2} \sin\left(\frac{3\pi z}{L}\right) \tag{40}$$

$$\varphi(z) = A_{\varphi 1} \sin\left(\frac{\pi z}{L}\right) + A_{\varphi 3} \sin\left(\frac{3\pi z}{L}\right). \tag{41}$$

The 1-term and 2-terms solutions are compared in Table 1 for a wide range of $\bar{k}$-values. The agreement improves as the number of fastener stations increase and the comparison is only shown for up to four fastener stations. As can be seen, the difference in buckling load (Δ) is less than 0.5% for all $\bar{k}$-values and for all fastener arrangements except two fastener stations, for which the maximum error is 2.66% and two or more terms are required in the displacement field for an accurate solution. For three or more fastener stations, the 1-term solution is highly accurate.

Table 1: Comparison of 1-term and 2-terms solutions for simply supported column free to warp at the ends

	Number	1 fastener station		2 fastener stations		3 fastener stations		4 fastener stations	
$\bar{k}$	of terms	P_{cr} (kN)	Δ	P_{cr} (kN)	Δ	P_{cr} (kN)	Δ	P_{cr} (kN)	Δ
0	3	130.320	0.00%	130.320	0.00%	130.320	0.00%	130.320	0.00000%
	6	130.320		130.320		130.320		130.320	
0.00001	3	130.562	0.00%	130.322	0.00%	130.564	0.00%	130.685	0.00000%
	6	130.562		130.322		130.564		130.685	
0.0001	3	132.664	0.00%	130.339	0.00%	132.682	0.00%	133.795	0.00000%
	6	132.665		130.339		132.683		133.795	
0.001	3	147.591	0.05%	130.511	0.00%	147.690	0.05%	152.982	0.00001%
	6	147.664		130.511		147.760		152.982	
0.01	3	174.178	0.25%	132.178	0.01%	174.261	0.23%	177.073	0.00002%
	6	174.607		132.186		174.662		177.073	
0.1	3	181.160	0.30%	144.473	0.32%	181.237	0.26%	182.010	0.00002%
	6	181.708		144.933		181.715		182.010	
1	3	181.955	0.31%	169.439	1.99%	182.221	0.16%	182.548	0.00001%
	6	182.517		172.810		182.518		182.548	
10	3	182.036	0.31%	176.896	2.59%	182.539	0.03%	182.602	0.00000%
	6	182.599		181.473		182.599		182.602	
100	3	182.044	0.31%	177.772	2.66%	182.601	0.00%	182.608	0.00000%
	6	182.607		182.493		182.608		182.608	

To investigate the dependency of the lateral deflections of the component beams on the fastener shear stiffness, Fig. 12 shows the ratio $u^{m_2}(\frac{L}{2})/u^{m_1}(\frac{L}{2})$ for increasing values of $\bar{k}$ based on the 1-term solution. The ratio is calculated from the eigenvector ($\{A_{u1}^{m_1}, A_{u1}^{m_2}, A_{\varphi 1}\}$) obtained from solving Eq. (22) as the ratio between $A_{u1}^{m_2}$ and $A_{u1}^{m_1}$. Recalling that u^{m_1} and u^{m_2} are the lateral displacements of the shear centres of the component sections m_1 and m_2, respectively, as shown in

Fig. 2c, it follows from Fig. 12 that for negligible fastener shear stiffness ($\bar{k} \to 0$), the ratio is negative, implying that the shear centre of section m_1 moves in the negative x-direction as the shear centre of m_2 moves in the positive x-direction. This occurs partly because the two sections become virtually free to slide relative to each other along the web interface and partly because the shear centre of m_1 lies below the shear centre of the built-up section whereby a twist rotation about the shear centre of the built-up section causes a displacement $u^{m_1}(\frac{L}{2})$ in the negative x-direction. As the fastener shear stiffness increases, the sliding is gradually prevented and the shear centre of m_1 moves in the positive x-direction. However, the $u^{m_1}(\frac{L}{2})$ displacement remains small (3.9% of $u^{m_2}(\frac{L}{2})$) with the $u^{m_2}(\frac{L}{2})/u^{m_1}(\frac{L}{2})$-ratio approaching 25.7 in the limit $\bar{k} \to \infty$, as shown in Fig. 12.

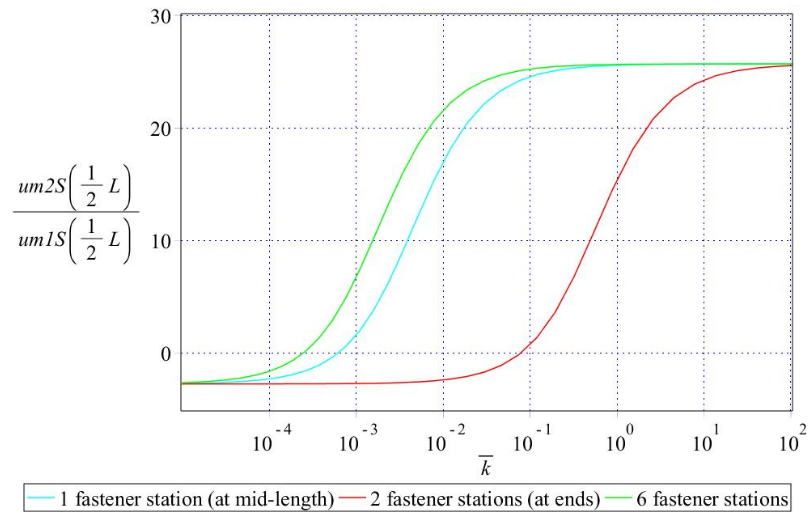

Figure 12: Ratio of lateral displacements at mid-length for simply supported built-up column with ends free to warp

3.3 Solution for a simply supported built-up column with loading applied through rigid end platens

We consider the same built-up column as that in Section 3.2 but change the end support conditions to be loading through pinned rigid end platens that prevent warping ($\varphi' = 0$) and enforce compatibility between the major axis rotations ($u^{m_1'}, u^{m_2'}$) of sections m_1 and m_2, as shown in Fig. 13a, i.e.

$$u^{m_1'} = u^{m_2'} \text{ at } z = 0 \text{ and } z = L\,. \tag{42}$$

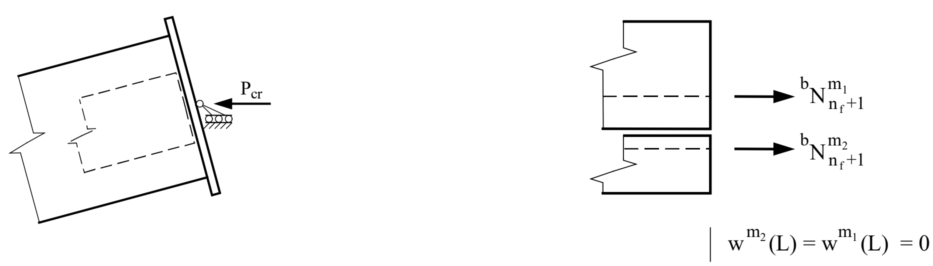

a) Loading through pinned rigid end platen. Plan view

b) Axial forces and relative longitudinal displacements at end cross-sections. Loading through rigid end platen. Side view

Figure 13: Loading through pinned rigid end platens

Because buckling occurs in the *xz*-plane, i.e. $v^{m_1} = v^{m_2} = v^{m_1'} = v^{m_2'} = 0$, the relative longitudinal displacement must be zero at the ends during buckling, so that,

$$w^{m_1} - w^{m_2} = 0 \text{ at } z = 0 \text{ and } z = L\,. \tag{43}$$

It would be possible for axial forces ($N_i^{m_1}$, $N_i^{m_2}$) to develop in the component sections during buckling and for equal but opposite axial forces to be transferred between the component sections through the rigid end platens. However, because no axial forces are transferred between the sections at the fastener stations (Eq. (32)), the axial force in each component section is constant along the length, and since the end displacements of the two sections are equal (Eq. (43)), the axial forces at the ends and along the members ($N_i^{m_1}$, $N_i^{m_2}$) must be zero. Consequently, as for the case of warping free end supports, the first term ($EA^{m_k}\, w^{m_k\prime}\, \delta w^{m_k\prime}$) of the energy equation (Eq. (15)) vanishes.

The solution is obtained for the following displacement field,

$$u^{m_1}(z) = A_{u1}^{m_1} \sin\left(\frac{\pi z}{L}\right) + \frac{A_{u2}^{m_1}}{2}\left(1 - \cos\left(\frac{2\pi z}{L}\right)\right) \tag{44}$$

$$u^{m_2}(z) = A_{u1}^{m_2} \sin\left(\frac{\pi z}{L}\right) + \frac{A_{u2}^{m_2}}{2}\left(1 - \cos\left(\frac{2\pi z}{L}\right)\right) \tag{45}$$

$$\varphi(z) = \frac{A_{\varphi 2}}{2}\left(1 - \cos\left(\frac{2\pi z}{L}\right)\right) + \frac{A_{\varphi 4}}{2}\left(1 - \cos\left(\frac{4\pi z}{L}\right)\right), \tag{46}$$

which satisfies the end support conditions. The solutions for the buckling load (P_{cr}) are shown in Fig. 14 relative to the buckling load ($P_{cr}(k{=}0)$) for the case $k = 0$, corresponding to no fasteners.

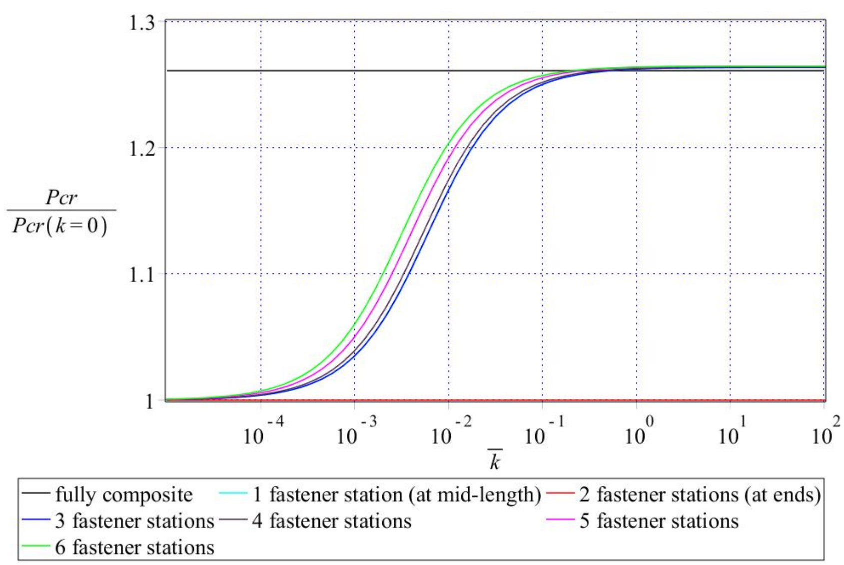

Figure 14: Nondimensional buckling load for simply supported built-up column with rigid end platens, ($P_{cr}(k{=}0) = 484.7$ kN)

It follows from Fig. 14 that the buckling load increases as the number of fastener stations increases, except for the case of two fastener stations, for which the solution is unaffected by the presence of fasteners at the ends. The latter result is a consequence of the warping restraint provided by the rigid end platens, which suppresses longitudinal shear deformations ($\Delta_{l,ij} = 0$) and renders the fasteners ineffective. For three or more fastener stations, the buckling load (P_{cr}) approaches 612.8 kN in the limit $\bar{k} \rightarrow \infty$. This result is within 0.3% of the buckling load (611.2 kN) obtained for the fully composite member, thus indicating the solutions are accurate. As for the case of warping free end supports, the results for one and three fastener stations are indistinguishable, and only a small fastener shear stiffness ($\bar{k} \approx 10^{-1}$) is required to achieve virtually full composite action for all fastener arrangements except fasteners installed at the ends.

4. Conclusions

The paper presents the flexural-torsional buckling analysis of a cold-formed steel built-up column with discrete fasteners along the length. The discrete locations of the fasteners are considered explicitly, in contract to alternative approaches based on smearing the shear stiffness of the discrete fastener over the length of the column. The buckling equation is first established and subsequently solved using an energy approach for two support conditions, *viz*. concentrically loaded columns with ends free to warp and columns loaded though rigid end platens preventing warping and enforcing compatibility between the major axis rotations of the two component sections.

The results demonstrate that the installation of fasteners leads to increases in buckling loads of 40.1% and 26.4% for columns free to warp at the ends and columns loaded through pinned rigid end platens, respectively, and that the increase can be achieved using only a small number of fasteners having only a modest shear stiffness. The results also show that the most effective location of fasteners is near the mid-length, where the maximum transverse shear deformations of the fasteners occur. This is the opposite to the case of the in-plane flexural buckling of pin-ended cold-formed steel columns for which fasteners have greatest effect near the ends when longitudinal shear deformations are allowed at the ends.

While the paper is concerned with the flexural-torsional buckling of singly symmetric cold-formed steel columns, in designing such columns, a separate analysis of the flexural buckling in the plane of symmetry will also be required, as will analyses of the local and distortional buckling loads.

Acknowledgments

The research described in this paper is supported by the Australian Research Council (ARC) Discovery Project DP220103573.

References

Abbasi, M., Rasmussen, K.J.R., Khezri, M. and Schafer, B.W. (2023). "Computational modelling of built-up cold-formed steel columns and parametric studies." *Thin–Walled Structures* 191.

AISI-S100 (2020). North American Specification for the Design of Cold-formed Steel Structural Members. Washington, D.C., American Iron and Steel Institute.

AS/NZS4600 (2018). Cold-formed Steel Structures. Sydney, Standards Australia.

Budiansky, B. (1974). Theory of Buckling and Post-Buckling Behavior of Elastic Structures. Advances in Applied Mechanics. C.-S. Yih, Elsevier. 14**:** 1-65.

Chen, B., Roy, K., Uzzaman, A., Raftery, G. and Lim, J.B.P. (2020). "Axial strength of back-to-back cold-formed steel channels with edge-stiffened holes, un-stiffened holes and plain webs." *Journal of Constructional Steel Research* 174: 106313.

Dobric, J., Gluhovic, N., Fric, N., Ruan, X., Bock, M. and Rossi, B. (2024). "Buckling strengths of cold-formed built-up cruciform section columns under axial compression " *Thin-Walled Structures* 200: 111879.

Fratamico, D.C., Torabian, S., Zhao, X., Rasmussen, K.J.R. and Schafer, B.W. (2018). "Experiments on the global buckling and collapse of built-up cold-formed steel columns." *Journal of Constructional Steel Research* 144(1): 65-80.

Georgieva, I., Schueremans, L., Pyl, L. and Vandewalle, L. (2012). "Experimental investigation of built-up double-Z members in bending and compression." *Thin-walled Structures* 53: 48-57.

Li , Q.-Y. and Young, B. (2022). "Experimental and numerical investigation on cold-formed steel built-up section pin-ended columns." *Thin-Walled Structures* 170: 108444.

Lu, Y., Zhou, T., Li, W. and Wu, H. (2017). "Experimental investigation and a novel direct strength method for cold-formed built-up I-section columns." *Thin-walled Structures* 112: 125–139.

Mahar, A.M., Jayachandran, S. and Mahendran, M. (2023). "Design of cold-formed steel built-up back-to-back columns subject to local-flexural interactive buckling." *Journal of Structural Engineering* 149(12).

Meza, F.J., Becque, J. and Hajirasouliha, I. (2020). "Experimental study of cold-formed steel built-up beams." *Journal of Structural Engineering* 146(7).

Phan, D.K. and Rasmussen, K.J.R. (2019). "Flexural rigidity of cold-formed steel built-up members." *Thin-Walled Structures* 140 438-449.

Phan, D.K., Rasmussen, K.J.R. and Schafer, B.W. (2021). "Tests and design of built-up section columns." *Journal of Constructional Steel Research* 181: 106619.

Phan, D.K., Rasmussen, K.J.R. and Schafer, B.W. (2022). "Numerical investigation of the strength and design of cold-formed steel built-up columns." *Journal of Constructional Steel Research* 193: 107276.

Rasmussen, K.J.R. (1997). "Bifurcation of locally buckled members." *Thin-Walled Structures* 28(2): 117-154.

Rasmussen, K.J.R., Khezri, M., Schafer, B.W. and Zhang, H. (2020). "The mechanics of built-up cold-formed steel members." *Thin-walled Structures* 154: 106756.

Roy, K., Ting, T.C.H., Lau, H.H. and Lim, J.B.P. (2018). "Effect of thickness on the behaviour of axially loaded back-to-back cold-formed steel built-up channel sections - Experimental and numerical investigation." *Structures* 16: 327-346.

Trahair, N. (1993). Flexural-torsional Buckling of Structures. London, E & FN Spon.

Yang, J., Luo, K., Wang, W., Shi, Y. and Li, H. (2024). "Research on the flexural buckling behavior of the cold-formed steel back-to-back built-up columns with Σ-section." *Engineering Structures* 302: 117404.

Zhang, J.-H. and Young, B. (2015). "Numerical investigation and design of cold-formed steel built-up open section columns with longitudinal stiffeners." *Thin-Walled structures* 89: 178–191.

Zhou, T., Li, Y., Wu, H., Lu, Y. and Ren, L. (2020). "Analysis to determine flexural buckling of cold-formed steel built-up back-to-back section columns." *Journal of Constructional Steel Research* 166: 105898.